Characterization of Polypyrrole-CdSe/CdTe Nanocomposite Films Prepared with an All Electrochemical Deposition Process

Shih-Yuan Lu* and I-Hsin Lin

Department of Chemical Engineering, National Tsing-Hua University, Hsin-Chu, Taiwan 30043, Republic of China

Received: December 3, 2002; In Final Form: March 3, 2003

An all electrochemical deposition process was developed to prepare the polypyrrole nanocomposite films containing multiple layers of CdSe and CdTe. The CdSe layer grew on top of polypyrrole in a Volmer−Weber mode leading to an increase in surface roughness, while the subsequent CdTe layer filled up the interisland space of the CdSe layer resulting in smoother surfaces. A complete coverage of CdTe over the CdSe layer significantly improved the photoluminescence performance of the composite film. This demonstrates that wider band gap materials (CdSe here) can be enhanced in photoluminescence performance with passivation of surface states offered by a narrower band gap material (CdTe here) provided that the lowest conduction band of the narrower band gap material is located higher in energy level than that of the wider band gap material. A top covering layer of polypyrrole not only further smoothed the surface but also further boosted the photoluminescence intensity of the nanocomposite film because of the enhanced radiative electron−hole recombination.

Introduction

Inorganic semiconductor materials of nanodimension have drawn much research attention in recent years because of their size-tunable optoelectronic properties arising from the quantum confinement effect. These materials, however, cannot be applied alone under most circumstances and need to be incorporated into other materials, often polymers, to acquire necessary processability and protection. Consequently, polymer/semiconductor nanocomposites have become a popular material form for applications of nanomaterials.[1,2]

The optoelectronic properties of inorganic semiconductor-containing polymer nanocomposites depend not only on the optoelectronic properties and characteristic dimension of the semiconductor material but also on those of the host polymer. Conducting polymers such as polypyrrole, polyaniline, and so forth are good candidates for serving as the host matrix for inorganic semiconductors in optoelectronic applications because of the relatively high conductivity, excellent stability, and good transparency of these polymers. Furthermore, their hole-conducting ability, when combined with the electron-conducting inorganic semiconductors, can increase the radiative electron−hole recombination rate so as to improve the optoelectronic performance of the inorganic semiconductor.[3]

For some inorganic semiconductor materials, such as CdSe and CdS, the passivation of nonradiative recombination sites existing on the material surface, with a wider band gap semiconductor to improve their photoluminescence performance, is also an important practice.[4,5] In this article, we developed an all electrochemical deposition process to fabricate polypyrrole nanocomposites containing multilayers of CdSe and CdTe to investigate how coating layer of CdTe (a narrower band gap material than CdSe) and covering layer of polypyrrole (a hole-conducting material) affect the optical properties of the CdSe layer.

Experimental Section

Preparation of Nanocomposite Films. The preparation of the CdSe/CdTe polypyrrole nanocomposite films was divided into three subprocedures: preparation of the electrode, electropolymerization of pyrrole monomers, and electrochemical deposition of CdSe/CdTe layers. For the electrode preparation, gold film of 35-nm thick was deposited onto mica {111} sheets of 10 mm by 15 mm in a vacuum evaporator of 10^{-6} Torr at a rate of 0.53 Å/s. The gold-covered mica (denoted as M/Au) was annealed in the evaporator at 250 °C for 12 h to preserve and enhance the {111} texture.[6]

Polypyrrole layer (denoted as PPy) was introduced onto M/Au to start the polypyrrole composite or onto M/Au/PPy/semiconductor layer to complete the nanocomposite preparation. The electrolyte consisted of 0.05 M $(CH_3)_4NBF_4$ and 0.1 M pyrrole monomer in acetonitrile.[7] We used M/Au or M/Au/PPy/semiconductor layer as the anode and Pt as the cathode. Polypyrrole was deposited onto the anode surface at a galvanostatic mode of 1.0 mA/cm^2 at room temperature through an oxidation reaction. The layer thickness was adjusted through deposition time. After the deposition, the deposited substrate (M/Au/PPy or M/Au/PPy/semiconductor layer/PPy) was dried and cooled in air to room temperature for 3 h to promote formation of oxidized state for the polypyrrole layer.

Layers of CdSe or CdTe were introduced onto relevant substrates by galvanostatic electrodeposition in a two-electrode cell with the substrate as the cathode and carbon as the anode. The electrolyte was made up of 50 mM $Cd(ClO_4)_2 \cdot 6H_2O$ and 12 mM elemental Se (or Te for deposition of CdTe layer) in dimethylsulfoxide and was heated to 120 °C before proceeding with the electrochemical deposition at 0.1 mA/cm^2.[8] The layer

* Corresponding author. Fax: 886-3-5715408; e-mail: sylu@che.nthu.edu.tw.

10.1021/jp022508p CCC: $25.00
Published on Web 06/25/2003

thickness was controlled by the deposition time. After deposition, the substrate was immersed into a hot dimethylsufoxide bath of 120 °C for several seconds to rinse away excessive reactants. The substrate was then dried in nitrogen and sealed in a sample box kept in dark to avoid possible oxidation. Before a CdTe layer was deposited, a layer of CdSe would always be deposited first. With this procedure, no elemental Se was needed to be present in the electrolyte as a promoter for deposition of CdTe layer.

Characterizations. *Optical Characterization.* A Hitachi U-3300 spectrophotometer was used to perform the absorption measurement. The slit was set at 2 nm and the scan rate at 120 nm/min. For photoluminescence spectroscopy, a Hitachi F-4500 equipped with a xenon lamp (150 W), a 700 V photomultiplier tube detector, and a solid sample holder was used to measure the photoluminescence of the solid film. Measurements were carried out with both the excitation and emission slits set at 10 nm and a scan rate at 240 nm/min. Both absorption and emission spectra were obtained at room temperature.

X-ray Photoelectron Spectroscopy. XPS was performed using a Physical Electronics PHI-1600 spectrometer equipped with a dual X-ray anode (Mg and Al), a spherical capacitor analyzer, and a multichannel detector. Data were obtained with Mg Kα radiation (1253.6 eV) at 400 W (15 keV). Survey scans were collected over the range 0−1100 eV with a 117 eV pass energy detection, corresponding to a resolution of 1 eV. Closeup scans were collected around the peaks of interest for the different elements with a 23.5 eV pass energy detection and a resolution of 0.2 eV. A base pressure of 10^{-10} Torr was maintained during the measurement. The energy scale was calibrated using C_{1s} (at 284.8 eV) as a reference.

Microscopy. Scanning electron microscopy (SEM) measurements were obtained with a Hitachi S-4700 operated at an accelerated voltage of 2 kV. It was equipped with a cathode electronic gun as the electron source. The secondary electron resolution was about 1.5 nm at 15 kV. All samples were sputtered with Au to form a thin layer of Au of around 2-nm thick before analysis. Atomic force microscopy (AFM) images were obtained with a Digital Instruments Nanoscope J in the contact mode.

Results and Discussion

Two layers of PPy films were deposited in the preparation of the nanocomposite film: one as the starting PPy layer and the other the top covering PPy layer. The deposition time was set at 5 and 20 s for the starting and covering PPy layers, respectively. The starting PPy layer in fact was only pyrrole oligomers for a deposition time of 5 s, as evidenced from the major UV−vis absorption peak between 293 and 338 nm (graph not shown here).[9] This pyrrole oligomer layer was thin (around 20 nm) and smooth enough to preserve the substrate crystalline texture for later size control for semiconductor crystals[10] and was also conducting enough to enable subsequent electrochemical deposition procedures.

Figure 1 shows the absorption spectra of the CdSe layer grown on top of the M/Au/PPy5s substrate. The absorbance of the M/Au/PPy5s substrate had been subtracted from the total absorbance, leaving roughly that for the CdSe layer. With increasing deposition time from 15 to 60 s, the CdSe nanocrystal grew larger resulting in a slight redshift in absorption peak away from 500 nm. The energy band gap of bulk CdSe at 300 K is 1.85 eV[11] corresponding to an absorption peak of 670 nm. The CdSe layer caused a substantial blueshift in the absorption spectra because of the quantum size confinement effect. The

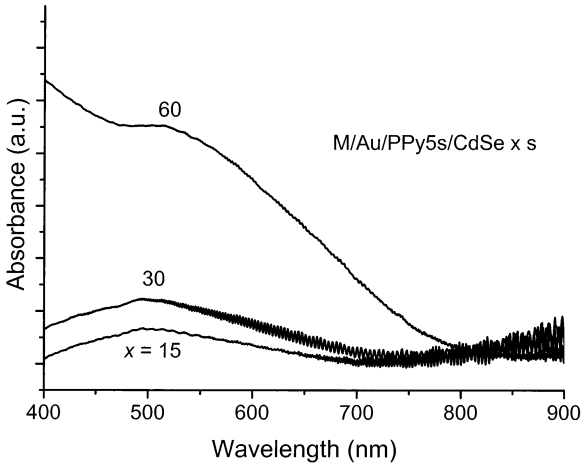

Figure 1. Absorption spectra of CdSe layers deposited with deposition times of 15, 30, and 60 s, showing a slight redshift in absorption peaks with increasing deposition time.

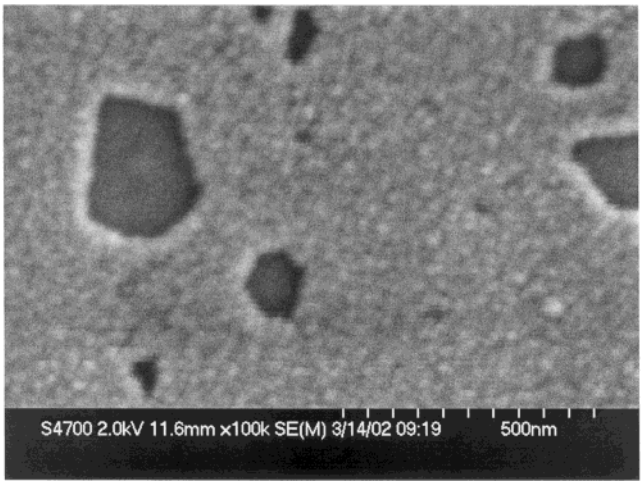

Figure 2. An SEM graph of the CdSe particle film prepared with a deposition time of 15 s.

absorption onset, however, occurred at wavelengths even longer than 670 nm. This peculiarity may be explained as follows. In addition to the major absorption peak between 293 and 338 nm, the PPy5s layer showed also a moderate absorption band starting from around 600 nm with an increasing intensity for longer wavelengths (data not shown here). This absorption band was enhanced with deposition of the CdSe layer, resulting in an overshoot in that wavelength band after the subtraction procedure for the absorption data acquisition of the CdSe layer. The longer than expected onset tail may be attributed to this nonrigorous subtraction procedure in obtaining absorption data for the CdSe layer. The absorption peaks appearing around 500 nm, however, were not influenced by this nonrigorous subtraction procedure.

Figure 2 shows the SEM graph for the M/Au/PPy5s/CdSe15s substrate. A CdSe particle film was formed because the CdSe grew in a Volmer−Weber mode (3-D island growth) on top of the PPy layer because of the large lattice mismatch between them. Figure 3 shows the absorption spectra of CdSe coated with different thickness of CdTe quantified as different deposition time of CdTe. Here, again, the absorption of the M/Au/PPy5s substrate was subtracted from the total absorption. The absorption peak shows a more pronounced redshift because of the influence of CdTe layer of increasing coverage. The energy band gap of bulk CdTe at 300 K is 1.51 eV[11] corresponding to an absorption peak of 821 nm.

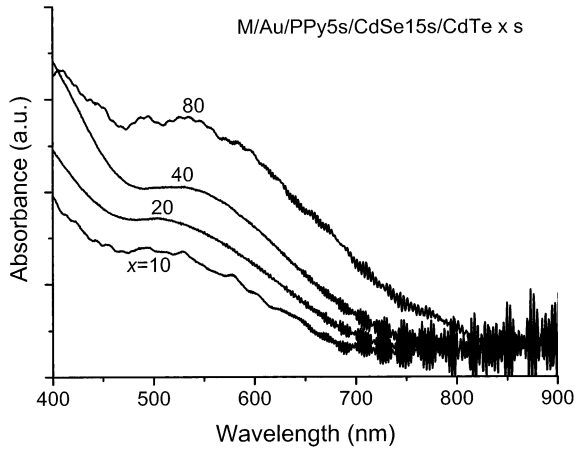

Figure 3. Absorption spectra of CdSe layers of a 15-s deposition time coated with a CdTe layer of increasing deposition from 10 to 80 s, showing a more pronounced redshift in absorption peaks with increasing deposition time of the CdTe layer.

To examine the covering and protecting ability of CdTe layer for CdSe layer, we purposely exposed M/Au/PPy5s/CdSE15s/CdTe substrates to air for 75 h and detected the formation of SeO_2 by XPS analyses. Here, CdTe layers were deposited at a series of different deposition times. From Figure 4a, the coexistence of CdSe and CdTe was clearly shown for a CdTe deposition of 5 s. When the CdTe deposition time was increased to 80 s, the Se related peaks disappeared leaving only Cd and Te related peaks. This shows a complete coverage of CdSe layer by CdTe layer. In Figure 4c, a closeup survey scan in the 50−65 eV range shows a clear peak diminishing process for Se and SeO_2 with an increasing deposition time for CdTe. At a deposition time of 80 s for CdTe, the Se and SeO_2 peaks completely disappeared implying a complete and effective coverage of CdTe over CdSe.

Here, appreciable alloy formation between the CdSe and CdTe layers seems to be unlikely for the following reasons. First, solid diffusion is an extremely slow process, although much sped up in nanoscale, and the highest processing temperature here was only 120 °C for a short period of time. In addition, the absorption spectra of CdSe after the deposition of CdTe layer were not significantly altered, implying no significant alloying has occurred.

The complete and effective coverage of CdSe with CdTe resulted in a significant enhancement in photoluminescence intensity for the composite film. As shown in Figure 5, the photoluminescence intensity of substrate M/Au/PPy5s/CdSe15s/CdTe20s remained almost the same with that of M/Au/PPy5s/CdSe15s implying a 20-s deposition of CdTe did not effectively passivate the surface states of CdSe and did not effectively protect CdSe from the attack of oxygen. But at a deposition time of 80 s for CdTe, an effective and a complete coverage of CdTe over CdSe was achieved leading to a significant increase in photoluminescence intensity. Also shown in the figure is the further boost in photoluminescence intensity provided by the covering PPy layer. This enhancing effect is believed to be due to the enhanced electron−hole recombination made possible by the presence of the hole-conducting PPy layer.

Figure 6 is a schematic energy level diagram for PPy, CdSe, and CdTe[11,12,13] that can be used to explain the trend in photoluminescence intensity observed in Figure 5. Among the three materials, the lowest conduction band of PPy (p-type as prepared in an electrochemical deposition process) is located the highest in the diagram, that of CdTe next, and that of CdSe

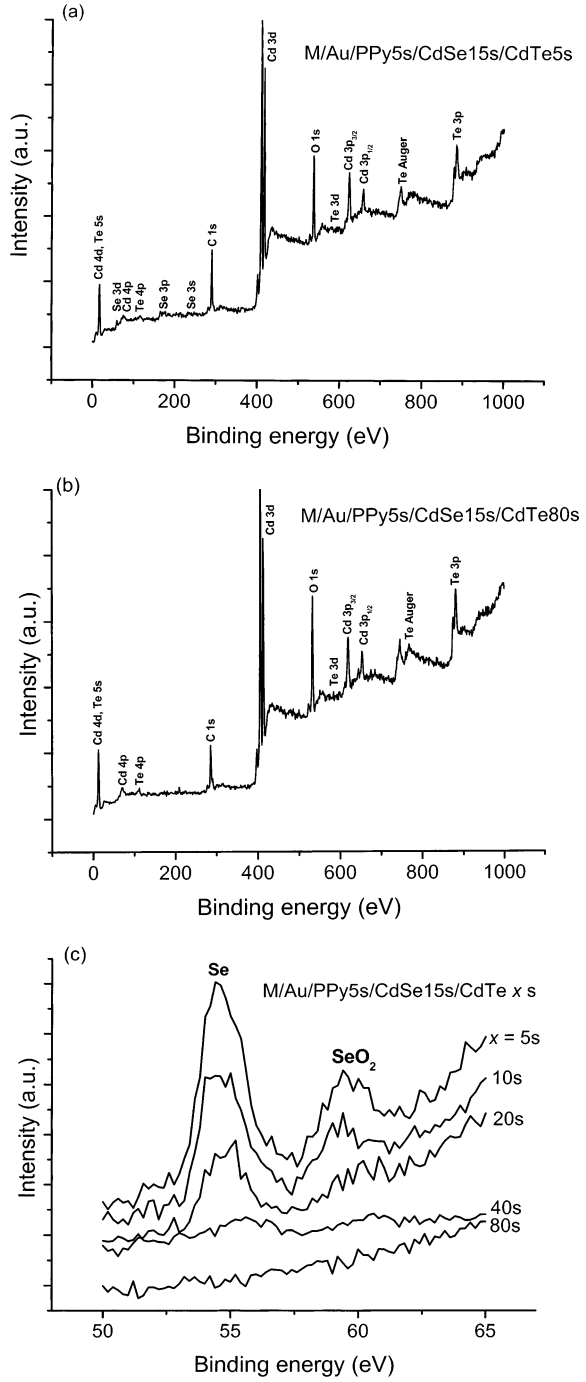

Figure 4. Survey spectra of (a) the M/Au/PPy5s/CdSe15s/CdTe5s substrate and (b) the M/Au/PPy5s/CdSe15s/CdTe80s substrate, showing the disappearance of Se signals after a deposition of 80 s CdTe layer. (c) Closeup survey spectra in the low-energy range of 50−65 eV, showing the diminishing of Se and SeO_2 peaks with increasing deposition time from 5 to 80 s for the CdTe layer.

the lowest. When CdSe is covered with CdTe, the excited electrons of CdTe can be transported to the conduction band of CdSe so to increase the electron−hole recombination efficiency and thus the photoluminescence intensity. Similarly, the excited electrons of the covering PPy layer can be transported to the conduction band of CdSe, together with the extra holes of the p-doped PPy layer, to further raise the photoluminescence intensity of the composite film.

The absorption peaks of the nanocomposite films fall in the range of 500−550 nm as shown in Figures 1 and 3, while their corresponding photoluminescence peaks are located in the 590−

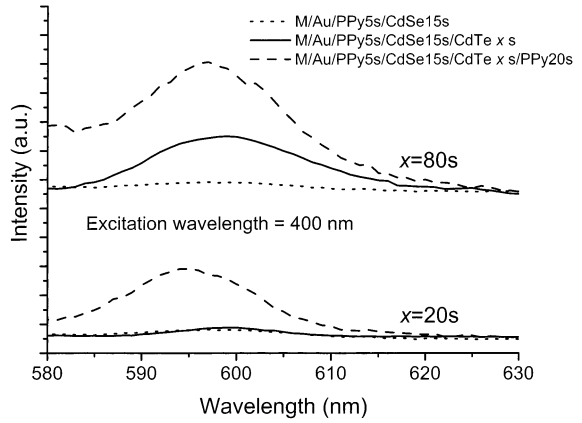

Figure 5. PL spectra for a sequential deposition of CdSe, CdTe, and PPy layers, showing a significant intensity boost at the complete coverage of CdTe on CdSe and a further enhancement resulting from the introduction of the PPy layer.

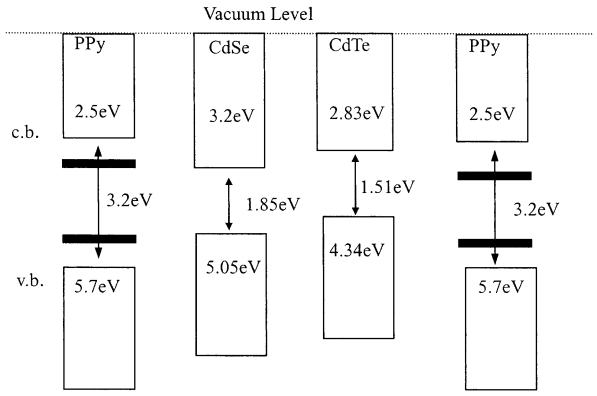

Figure 6. Schematic energy level diagram for PPy, CdSe, and CdTe, showing the relative position of their lowest conduction bands in the order of PPy, CdTe, and CdSe from high to low.

600 nm range with a peak span of less than 40 nm. The near-band-edge luminescence becomes pronounced as the CdTe layer coverage gets more complete. The introduction of the PPy covering layer caused a slight blueshift in the photoluminescence peak.

It is also interesting to see how an additional CdSe layer deposited on top of the CdTe layer would affect the photoluminescence intensity of the nanocomposite film. Figure 7 shows the decreasing trend in photoluminescence intensity caused by the increasing deposition time of the second CdSe layer. This phenomenon may be due to the increasing amount of defects and surface states accompanying the introduction of the second CdSe layer.

Table 1 tabulates the mean surface roughness of the film as determined from AFM data over a surface area of at least 1 μm by 1 μm. Information about the morphology evolution along subsequent deposition and layer growth mode can be inferred from this table. First, the smoothness of PPy layer was conformed with the small roughness of 5-s PPy deposition. With the deposition of 15-s CdSe, the roughness significantly increased to 9.6 nm indicating a Volmer−Weber (3-D island) growth mode for CdSe on PPy. A covering PPy layer of 20-s deposition reduced the roughness to 4.3 nm by filling up the interisland space of the CdSe layer. The reduction in roughness for M/Au/PPy5s/CdSe15s by a CdTe layer of 5 s was not as dramatic as that by the PPy layer of 20 s but was large enough to indicate the layer-by-layer growth of CdTe on CdSe to smooth out the original roughness created by the island growth mode

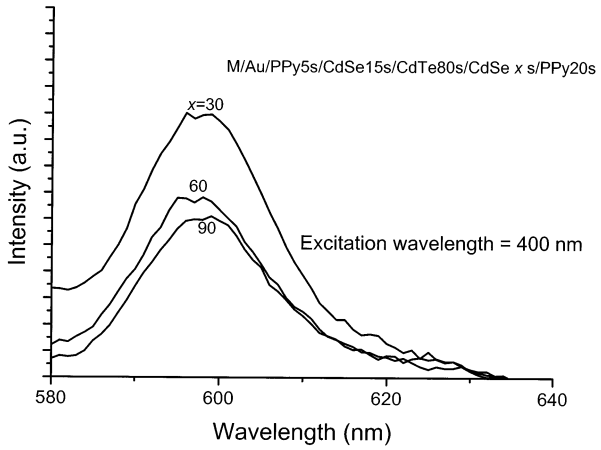

Figure 7. PL spectra for the M/Au/PPy5s/CdSe15s/CdTe80s/CdSe × s/PPy20s substrate with an increasing deposition time for the second CdSe layer from 30 to 90 s, showing a decreasing trend in PL intensity with increasing thickness of the second CdSe layer.

TABLE 1: Roughness Evolution with Progressing Electrochemical Deposition

substrate	mean roughness (nm)[a]
M/Au/PPy5s	1.1
M/Au/Ppy5s/CdSe15s	9.6
M/Au/Ppy5s/CdSe15s/Ppy20s	4.3
M/Au/Ppy5s/CdSe15s/CdTe5s	7.8
M/Au/Ppy5s/CdSe15s/CdTe80s	7.6
M/Au/Ppy5s/CdSe15s/CdTe5s/Ppy20s	5.0
M/Au/Ppy5s/CdSe15s/CdTe80s/Ppy20s	5.2

[a] AFM measurement over an area of at least 1 μm by 1 μm.

of CdSe on PPy. The roughness remained at the same level even if a much longer deposition time (80 s) of CdTe was used, providing a strong evidence that CdTe grew in a layer-by-layer mode. A further reduction on roughness was achieved by deposition of the covering PPy layer for both CdTe5s and CdTe80s substrates, and the resulting roughnesses were in the same order of magnitude.

Conclusion

An all electrochemical deposition process was successfully developed to fabricate nanocomposite films of polypyrrole containing multilayers of CdSe and CdTe. The relative location of the lowest conduction band, instead of the relative width of the energy band gap, plays the determining role on whether a coating layer can enhance the photoluminescence intensity of the coated layer. Also important is the completeness in coating coverage. A complete coverage of CdSe by CdTe is necessary to realize the desired enhancement in photoluminescence intensity. The surface roughness evolution also helped us determine layer growth mode of CdSe on PPy and CdTe on CdSe.

Acknowledgment. The authors gratefully acknowledge the support of the National Science Council of the Republic of China under grant NSC 90-2214-E-007-003. The authors also thank Prof. Show-An Chen of our department for his generosity in providing the Au deposition facility and Prof. C. -S. Liao of Yua-Ze University for the helpful discussion.

References and Notes

(1) Caseri, W. Macromol. *Rapid Commun*. **2000**, *21*, 705.
(2) Rajeshwar, K.; de Tacconi, N. R.; Chenthamarakshan, C. R. *Chem. Mater*. **2001**, *13*, 2765.
(3) Gaponik, N. P.; Talapin, D. V.; Rogach, A. L.; Eychmuller, A. *J. Mater. Chem*. **2000**, *10*, 2163.

(4) Peng, X. G.; Schlamp, M. C.; Kadavanich, A. V. *J. Am. Chem. Soc*. **1997**, *119*, 7019.
(5) Dabbousi, B. O.; Rodriguez-Viejo, J.; Mikulec, F. V.; Heine, J. R.; Mattoussi, H.; Ober, R.; Jensen, K. F.; Bawendi, M. G. *J. Phys. Chem. B* **1997**, *101*, 9463.
(6) Golan, Y.; Margulis, L.; Rubinstein, I. *Surf. Sci.* **1992**, *264*, 312.
(7) Valaski, R.; Ayoub, S.; Micaroni, L.; Hümmelgen, I. A. *Thin Solid Films* **2001**, *388*, 171.
(8) Golan, Y.; Margulis, L.; Rubinstein, I.; Hodes, G. *Langmuir* **1992**, *8*, 749.
(9) Appel, G.; Schmeiber, D.; Bauer, J.; Bauer, M.; Egelhaaf, H. J.; Oelkrug, D. *Synth. Met.* **1999**, *99*, 69.
(10) Golan, Y.; Alperson, B.; Hutchison, J. L.; Hodes, G.; Rubinstein, I. *Adv. Mater.* **1997**, *9*, 236.
(11) *Semiconductor Materials*; Berger, L. I.; CRC Press: New York, 1997.
(12) Cassagneau, T.; Mallouk, T. E.; Fendler, J. H. *J. Am. Chem. Soc.* **1998**, *120*, 7848.
(13) Wei, S.-H.; Zang, S. B.; Zunger, A. *J. Appl. Phys.* **2000**, *87*, 1304.